El Niño-Southern Oscillation (ENSO) since A.D. 1525

integrating evidence from tree-ring, coral, ice and documentary archives

Joëlle Gergis[1,2], Anthony Fowler[2], Karl Braganza[3], Scott Mooney[1] & James Risbey[4]

[1] School of Biological, Earth and Environmental Sciences, University of New South Wales, Kensington, 2052, Sydney, Australia, [2] Tree-ring Laboratory, School of Geography and Environmental Science, University of Auckland, Private Bag 92019 Auckland, New Zealand,

[3] National Climate Centre, Bureau of Meteorology, Melbourne GPO Box 1289K, Melbourne Victoria 3001, Australia, [4] Centre for Dynamical Meteorology and Oceanography, School of Mathematical Sciences, Monash University, PO Box 28M Clayton, Victoria 3800, Melbourne, Australia.

How to define ENSO for proxy calibration??

ENSO (El Niño–Southern Oscillation) is the largest source of inter-annual variability operating in the Earth's climate system. Nevertheless, no consensus exists within the scientific community as to which index best characterises large-scale (rather than regional) ENSO events. Atmospheric & oceanic components of ENSO can be out of phase & the magnitude of event anomalies can differ considerably (**Figure 1**). As a result, proxy records that have transfer functions derived from either index may fail to register these 'decoupled' events, potentially resulting in a fragmented description of past ENSO conditions from palaeoclimate archives.

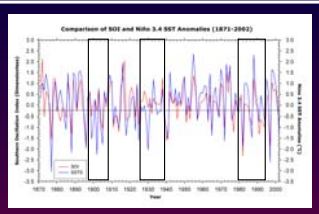

Figure 1. Comparison of Southern Oscillation Index (SOI) and Niño 3.4 region SSTs, 1871–2003. Note SSTs have been inverted to correspond with the SOI. Black boxes indicate periods when the atmosphere and ocean were out of phase, or indeed, indicated opposite conditions e.g. ~1930s.

Coupled ENSO Index (CEI)

The Coupled ENSO Index (CEI) is a composite, instrumental index of ENSO designed for the calibration of high-resolution proxy records. The CEI simultaneously identifies BOTH oceanic (Niño 3.4 region SSTs) and atmospheric (Southern Oscillation Index) anomalies for the instrumental period (1872–2002). Importantly, decoupled and lead/lag ENSO characteristics indicated by a sole index are preserved, while synchronous (coupled) events are registered as an amplification of magnitude (**Figure 2**).

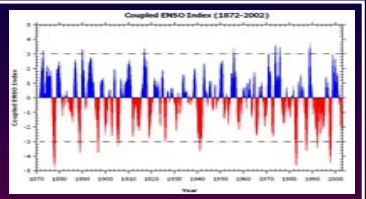

Figure 2. Coupled ENSO index (CEI), 1872–2002, constructed using the Southern Oscillation Index (SOI) smoothed with 11 month running mean and inverted Niño 3.4 region SSTs (NOAA post-1949 data, pre-1950 Trenberth reconstruction data) smoothed with 5 month running mean. Interestingly, the post-1970 period contains 50% of all extremes ENSO episodes observed from the observational period (Gergis & Fowler, International Journal of Climatology, *in press-September*).

3,727 years of ENSO from a regional West Pacific proxy; New Zealand Kauri

Figure 5. (left) Kauri's modern geographical range, North Island New Zealand. There are now 17 individual sites incorporated into the modern master Kauri chronology derived from living trees.

Figure 6. (right) Huge swamp Kauri preserved in bogs has extended the record back for the past 4 millennia from 11 individual sub-fossil sites.

Kauri is among a handful of tree species in the world which contains an identified "ENSO signal" in its growth ring patterns (**Figure 3**). They can reach heights of 30m (98ft), girth sizes greater than 10m (33 ft) and ages in excess of 2,000 years (**Figure 4**). Ancient Kauri are also found preserved in swamps of New Zealand (**Figures 5 & 6**).

Currently, chronologies derived from living trees & swamp material continuously span 3,727 years (1724 B.C. – A.D.2002). This makes the Kauri record the longest ENSO sensitive tree-ring record from the 'data sparse' Western Pacific, & indeed, the world.

Figure 4. (above) The Yakkas tree in Waipoua forest is one of the largest remaining trees in New Zealand: it has a diameter at breast height (DBH) of 4.65m. This tree was not sampled.

Figure 3. (below) Seasonal response function of Kauri growth with temperature (red), precipitation (blue) and the SOI (black). Strongest signal is in the austral spring (shaded). Dashed (solid) lines high (low) pass filtered. i.e. K020 (K200)

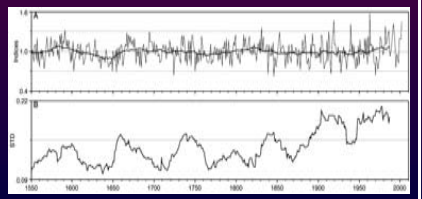

Figure 7. (above) Excerpt of the Kauri chronology, A.D. 1550–2002. Plot A shows a low pass filtered version of the tree ring-width chronology (50% variance cut off at 200 years). Plot B shows 31-year sliding variance plot to highlight variability through time.

Analysis of the modern master record (**Figure 7**) shows a remarkable shift in variance at ~1870 (coincident with the end of the Little Ice Age and global industrialisation) & a prominent 50–70 year cycle. From Kauri, the late C20th appears unusual in the context of the past 450yrs.

Multiproxy approaches to ENSO reconstruction; integrating regional signals

Using multiple proxies allows large-scale ENSO to be investigated, revealing how individual episodes varied spatially across the equatorial Pacific core zone & key teleconnection areas (**Figure 8**).

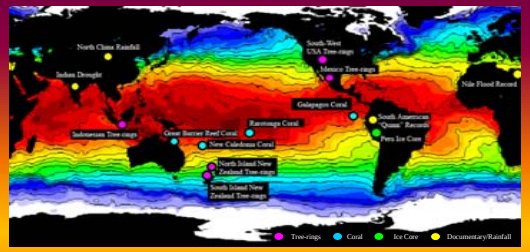

Figure 8. (above) Indicates the distribution of proxy records used in this study superposed on SST anomalies associated with the1997/98 El Niño event. All records selected based on published ENSO sensitivity & continuous record length.

1. Principal Component Analysis

Regressing dominant PCs against instrumental indices of ENSO (CEI, SOI & Niño 3.4 SSTs) including lead (t–1) and lag (t+1) relationships (**Figure 9**), revealed the multiproxy network best predicted peak ENSO maturity observed during the austral summer (DJF) represented by the Coupled ENSO Index (CEI) (**Figure 10**). Model verification indicated good reconstruction quality even with loss of records back in time (**Figure 11**).

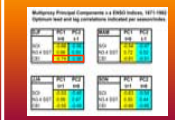

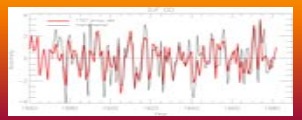

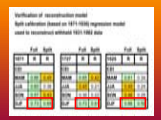

Figure 9. (left) Results of regressing multiproxy PC 1 and PC 2 with instrumental ENSO indices including lead & lag relationships, 1871–1982.
Figure 10. (middle) Comparison of instrumental DJF Coupled ENSO Index (CEI) (black) as predicted by the multiproxy regression model (red).
Figure 11. (right) Split calibration analysis to verify model performance; 1871–1930 model applied to withheld 1931–1982 data.

Figures 12 & 13 indicate a period of weakened ENSO activity in the 17th and 18th centuries, coincident with the broadly defined Little Ice Age and Maunder Minimum period of low solar activity is observed. Although extreme events are seen throughout reconstruction (**Figure 14**), the frequency of late C20th extremes appears unprecedented in the context of the past 500 years.

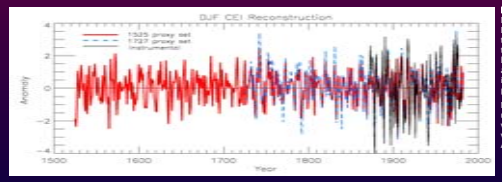

Figure 12. (left, top) Multiproxy reconstruction of ENSO since A.D. 1525. Red time series represents all tree-ring and ice records, blue reconstruction includes all coral sequences, with instrumental DJF CEI over plotted in black.

Note that a) reconstruction underestimates instrumental variability, b) late C20th variability unmatched since A.D. 1525,

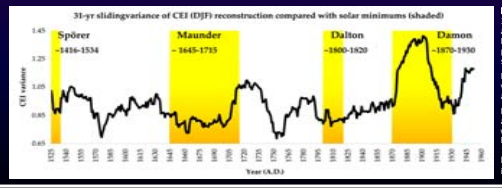

Figure 13. (left, bottom) 31yr sliding variance of austral summer (DJF) CEI ENSO reconstruction with periods of low solar activity shaded.

Note a decrease in ENSO variance during the Maunder and Dalton solar minimums.

Interestingly, the most active ENSO period coincides with the timing of the Damon minimum (~1870–1930) coincident with the beginning of large-scale industrialisation.

2. Discrete Event Analysis

Information about the occurrence and magnitude of past ENSO events is useful as a independent tool for cross-validation/verification of proxy and/or model reconstructions (Gergis and Fowler, *in prep*).

Calibrating proxy records using percentile analysis (all outliers maintained) revealed considerable differences in phase sensitivity, resulting in separate El Niño & La Niña reconstructions (**Table 1**). Since A.D. 1525, 92 El Niño & 82 La Niña events were reconstructed (**Table 2**). Decadal analysis (**Figure 14**) revealed the C20th contains 55% (25%) of all extreme El Niños (La Niñas) since A.D. 1525.

Compared to the 'Quinn records' of past El Niño events from South America, the list includes;

1. La Niña events
2. Range of (quantified) event magnitudes
3. Widespread East & West Pacific proxy data coverage
4. Reconstruction quality included (proxy skill)

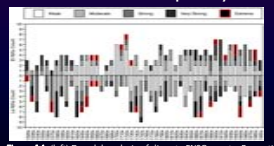

Figure 14. (left) Decadal analysis of discrete ENSO events. Percentile based magnitude classes ranging from weak-extreme.

Table 1. (right) Percentile based proxy calibration results. Each record is assessed using 'proxy skill' which reflects the ratio of accurate event capture v.s incorrect event detection (false positives). Note that considerable differences in phase sensitivity resulted in separate El Niño and La Niña reconstruction

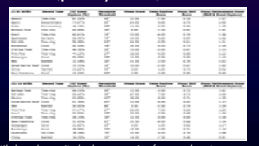

Table 2. ENSO events since A.D. 1525 Event list includes; Proxy Ratio (PR), Mean skill (MS), quality adjusted magnitude (MQ) score, & magnitude class (MC) from weak to extreme.

Acknowledgements: J.L.G would like to thank PAGES, the Asia-Pacific Network, the Chinese Academy of Sciences and the National Natural Science Foundation of China for generous financial assistance to attend the PAGES Open Science Meeting, Beijing, August 2005.